Millennial-scale isotope records from a wide-ranging predator show evidence of recent human impact to oceanic food webs

Anne E. Wiley[a,b,1], Peggy H. Ostrom[a], Andreanna J. Welch[c,d,e], Robert C. Fleischer[c], Hasand Gandhi[a], John R. Southon[f], Thomas W. Stafford, Jr.[g,h], Jay F. Penniman[i], Darcy Hu[j], Fern P. Duvall[k], and Helen F. James[b]

[a]Department of Zoology, Michigan State University, East Lansing, MI 48824; [b]Division of Birds, Department of Vertebrate Zoology, National Museum of Natural History, Smithsonian Institution, Washington, DC 20004; [c]Center for Conservation and Evolutionary Genetics, Smithsonian Conservation Biology Institute, National Zoological Park, Washington, DC 20008; [d]Behavior, Ecology, Evolution and Systematics Program, University of Maryland, College Park, MD 20742; [e]Department of Biological Sciences, University at Buffalo, Buffalo, NY 14260; [f]Department of Earth System Science, University of California, Irvine, CA 92617; [g]Department of Physics and Astronomy, University of Aarhus, DK-8000 Aarhus, Denmark; [h]Centre for GeoGenetics, Natural History Museum of Denmark, DK-1350 Copenhagen Denmark; [i]Pacific Cooperative Studies Unit, University of Hawaii, Honolulu, HI 96822; [j] Pacific West Regional Office, National Park Service, Honolulu, HI 96850; and [k]Department of Land and Natural Resources, Wailuku, HI 96793

Human exploitation of marine ecosystems is more recent in oceanic than near shore regions, yet our understanding of human impacts on oceanic food webs is comparatively poor. Few records of species that live beyond the continental shelves date back more than 60 y, and the sheer size of oceanic regions makes their food webs difficult to study, even in modern times. Here, we use stable carbon and nitrogen isotopes to study the foraging history of a generalist, oceanic predator, the Hawaiian petrel (*Pterodroma sandwichensis*), which ranges broadly in the Pacific from the equator to near the Aleutian Islands. Our isotope records from modern and ancient, radiocarbon-dated bones provide evidence of over 3,000 y of dietary stasis followed by a decline of ca. 1.8‰ in $\delta^{15}N$ over the past 100 y. Fishery-induced trophic decline is the most likely explanation for this sudden shift, which occurs in genetically distinct populations with disparate foraging locations. Our isotope records also show that coincident with the apparent decline in trophic level, foraging segregation among petrel populations decreased markedly. Because variation in the diet of generalist predators can reflect changing availability of their prey, a foraging shift in wide-ranging Hawaiian petrel populations suggests a relatively rapid change in the composition of oceanic food webs in the Northeast Pacific. Understanding and mitigating widespread shifts in prey availability may be a critical step in the conservation of endangered marine predators such as the Hawaiian petrel.

fishing | seabird | stable isotope

Historical baselines are a prerequisite to understanding the extent of human impact on a species or ecosystem. In coastal marine environments, retrospective studies show that habitat destruction and harvest of marine organisms have caused severe modifications, including trophic cascades and the regional loss of entire ecosystems (1, 2). It is difficult to assess the extent to which such impacts extend beyond continental shelves to the oceanic zone, because few chronological data are available for regions far out at sea, and the vast size of these ecosystems makes their food webs difficult to study, even in the present.

In the oceanic Northeast Pacific, significant human presence began with the colonization of the Hawaiian Islands, less than 1,000 y ago (3, 4). For centuries afterward, anthropogenic impacts, such as harvesting of marine organisms, were concentrated near the Islands; only in the 20th century, with the advent of industrialized fishing, have a wide variety of oceanic organisms been exploited at a broad spatial scale (5, 6). Our understanding of how human actions such as fishing have affected oceanic food web structure is primarily derived from catch statistics, which show a temporal decline in the abundance of some targeted groups, such as tuna, and in the trophic level of global catch (6–8). However, catch statistics can be strongly affected by shifting technologies and markets, and reflect only the abundance of species that are harvested. Moreover, catch statistics cannot record information about prehuman conditions, and very few systematically collected catch statistics or scientific surveys predate 1950.

Historical records from generalist predators offer an alternative means of studying marine food webs. Responding to changes in prey availability by shifting their diet or foraging locations, or else declining in abundance, predators such as seabirds can forage over large expanses and are often viewed as sentinels of their food webs (9–11). Here, we present millennial-scale records of foraging ecology from a wide-ranging, generalist predator, the Hawaiian petrel (*Pterodroma sandwichensis*), to provide a unique proxy for the condition of oceanic food webs in the Northeast Pacific Ocean. Shifts in Hawaiian petrel foraging habits have the potential to reflect changes occurring over large portions of the oceanic Pacific given the birds' diverse diet of fish, squid, and crustaceans; the high mobility of individuals (>10,000 km foraging trips); and the species' extensive range from the equator to near the Aleutian Islands (0–50°N, 135–175°W) (12–14).

Hawaiian petrels breed only on the main Hawaiian Islands, where their bones are abundant in paleontological and archaeological sites (Fig. 1). Within those bones, a record of petrel foraging locations and trophic level is preserved by stable carbon and nitrogen isotope values ($\delta^{13}C$ and $\delta^{15}N$) of the protein collagen (15, 16). We collected isotope data from over 250 individuals, including birds from every known modern and ancient Hawaiian petrel population. Equally extensive genetic studies (based largely on the same set of individuals) show that despite their high mobility, Hawaiian petrels rarely move between islands, and breeding colonies on different islands have diverged into genetically distinct populations (17, 18). Because at least some of those populations also have distinct foraging habits (15), we construct separate isotopic chronologies for each island population. Collectively, our chronologies extend back roughly
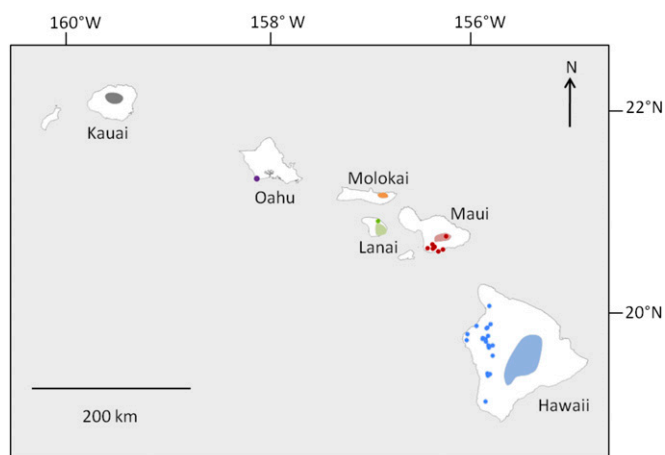
Fig. 1. Collection sites for Hawaiian petrel subfossil bones (dark-colored points), historic breeding distribution for the potentially extirpated population on Molokai, and modern breeding distribution on Kauai, Lanai, Maui, and Hawaii (lighter colored shapes). The distribution on Hawaii includes the saddle region between Mauna Kea and Mauna Loa, where Hawaiian petrel breeding is only documented by indigenous knowledge and bones (46, 58).

4,000 y, to well before human presence in the oceanic Northeast Pacific (3, 4). Our study therefore provides a unique, fishery-independent window into potential anthropogenic alterations of oceanic food webs.

Results and Discussion

We conducted a species-wide study of the Hawaiian petrel based on stable isotope data from six populations and two tissues: collagen and flight feather. Collagen is ideal for constructing long-term isotope chronologies, not only because it is preserved in ancient bones, but because its slow turnover rate in living birds results in an isotopic composition that can reflect foraging over a period of years (19). For the Hawaiian petrel, collagen data also provide spatially integrated dietary signals from individuals that are capable of traveling over large portions of the Northeast Pacific ocean, even within a single season (13). In contrast, flight feathers grow in a month or less during either the breeding season (for hatch-year birds) or nonbreeding season (for adults) (12, 15). Isotope data from flight feathers are therefore more useful for showing the diversity of foraging strategies present among Hawaiian petrels during short periods of time. Here, we study the isotopic composition of modern flight feathers to understand spatial and seasonal variation in petrel foraging habits and to aid in interpretation of our isotope chronologies from collagen.

We found large disparities in feather $\delta^{15}N$ and $\delta^{13}C$ values among populations and age groups, which we interpret as reflecting mainly divergences in foraging locations (Fig. 2, Table S1), as did Wiley et al. (15) in a study of two Hawaiian petrel populations. Our spatial interpretation of feather data is based on well-recognized $\delta^{15}N$ and $\delta^{13}C$ gradients within the Hawaiian petrel's distribution (Fig. 2A) (15), and is supported by observational studies. In brief, multiple data sets indicate that throughout North Pacific food webs, $\delta^{13}C$ varies inversely with latitude and $\delta^{15}N$ values decline precipitously away from an area of elevated $\delta^{15}N$ values in the southeast portion of Hawaiian petrel distribution, between 4–10° N and 135–140°W (20–24). Thus, petrels that focus their foraging southeast of the Hawaiian Islands are expected to have relatively high $\delta^{13}C$ and $\delta^{15}N$ values. Alternatively, the relatively high $\delta^{15}N$ values, such as those we observed for Lanai and Hawaii populations, could be due to feeding at a higher trophic level than other petrels. However, Laysan albatross (*Phoebastria immutabilis*) feeding north of the Hawaiian Islands, away from

the region of elevated $\delta^{15}N$, have relatively low $\delta^{15}N$ values (12.5‰) (15). Because Hawaiian petrels are unlikely to forage at a higher trophic level than the related and substantially larger Laysan albatross, $\delta^{15}N$ values greater than 12.5‰ in Hawaiian petrel feathers must result from feeding in a region of elevated $\delta^{15}N$.

High $\delta^{13}C$ values among adults are consistent with all adults growing feathers in the southern portion of Hawaiian petrel distribution, with variable $\delta^{15}N$ indicating that populations rely to different extents on areas of elevated $\delta^{15}N$ (e.g., in the southeast portion of the species' distribution; Fig. 2A). Relatively low $\delta^{13}C$ values of Maui and Kauai hatch-year birds are consistent with parental foraging trips near and north of the Hawaiian Islands, as shown by satellite tracks from Maui petrels (Fig. 2). In contrast, petrels from Hawaii likely provision their chicks with prey from southeast of the Hawaiian Islands, based on the elevated $\delta^{15}N$ and $\delta^{13}C$ values in the feathers of Hawaii hatch-year birds. Our interpretations of feather data are supported by multiple observational studies. For example, petrels breeding on Hawaii visit their nests more frequently than petrels on Maui, presumably due to shorter foraging trips to different at-sea locations (12, 25). In addition, at-sea observations show that Hawaiian petrels are more concentrated to the southeast of the Hawaiian Islands from October to December (the late breeding season and early nonbreeding season) than during the midbreeding season, consistent with our interpretation that adult petrels move toward this area during the early nonbreeding season (14). Overall, feather data show substantial variation in foraging location, both seasonally and among populations. In contrast, neither $\delta^{15}N$ nor $\delta^{13}C$ values of bone collagen vary significantly among modern petrel populations (comparisons of collagen $\delta^{15}N$ among populations can be found in Table S2; ANOVA for $\delta^{13}C$, $P = 0.597$, $F = 0.8434$, df = 11). Isotopic signals of location are apparently averaged out in modern bone collagen, likely due to the long time period represented by this tissue and the extensive foraging range of individual birds over the course of the breeding and nonbreeding seasons, combined.
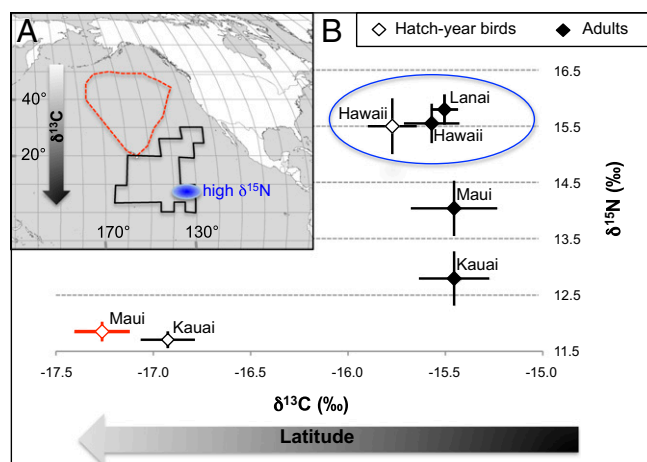
Fig. 2. Flight feather isotope data and at-sea locations of Hawaiian petrels. In A, the black line marks Hawaiian petrel distribution from transect surveys (14). The red dashed line is a typical flight path from a satellite-tracked Maui bird during the breeding season (13). These two regions represent the predominate areas where Hawaiian petrels occur. In A, the blue oval denotes an approximate area where organic matter and consumers have unusually high $\delta^{15}N$ values within the Hawaiian petrel's range (23, 24). In B, the blue circle identifies petrels that apparently concentrate their foraging in a region with elevated $\delta^{15}N$. In both panels, arrows emphasize the negative relationship between latitude and $\delta^{13}C$ of marine organisms (20–22). Hatch-year birds from Maui are outlined in red to associate them with the Maui flight path.

To evaluate temporal trends in foraging, we first grouped collagen samples into island populations: a grouping that allowed separate examination of genetically distinct populations with disparate foraging locations. Next, we divided collagen samples into time bins and compared average isotope values using ANOVA and Tukey honestly significant difference (HSD) post hoc tests (Fig. 3, Table S2). The initial time bins are based on archaeological chronology in the Hawaiian Islands, which were the population center for people fishing within the oceanic range of the Hawaiian petrel until historical times (in contrast, aboriginal people living on continents concentrated their fishing in nearshore environments of the continental shelves) (3, 5). The later time bins reflect the Historic period of Western economic development and whaling in Hawaii and the oceanic eastern North Pacific, followed by the Modern period of industrialized fishing.

Our isotope chronologies show that $\delta^{15}N$ disparities among populations have decreased through time. Before the Historic period, $\delta^{15}N$ values of bone collagen differ by as much as 2‰ and show statistically significant separation (Fig. 3, Table S2). In contrast, isotopic segregation is only observable among modern populations over the short time scales represented by flight feathers. This isotopic convergence of populations may be related to a seemingly concurrent, species-wide shift in $\delta^{15}N$ values.

Between the Prehuman and Modern periods, we observed significant $\delta^{15}N$ declines for petrel populations on Lanai, Maui, and Hawaii (all of the populations from which modern samples were available) (Fig. 3, Table S2). $\delta^{15}N$ values from the sample-rich Hawaii chronology did not decline until sometime after the early Expansion period ($P < 0.01$ for Expansion vs. Modern periods, $P = 0.44$ for Prehuman vs. Expansion periods). The 10 most recent Expansion period samples from Hawaii (average age = 204 B.P.) had an average $\delta^{15}N$ of 16.8 ± 0.5‰, which is similar to the average $\delta^{15}N$ of the remaining samples in this time period (16.5 ± 0.1‰) and implies that the $\delta^{15}N$ decline occurred after ca. 200 B.P. Petrels collected on the island of Molokai in 1914 have an average $\delta^{15}N$ value that does not differ significantly

from that of any ancient population ($P = 0.072$ for Prehuman Hawaii, $P > 0.76$ for all other comparisons), but is higher than the $\delta^{15}N$ of modern Maui and Lanai populations (Table S2), suggesting that $\delta^{15}N$ decline occurred within the past 100 y. Notably, the decline in $\delta^{15}N$ between ancient and modern petrels is a robust characteristic of our timelines: it is present regardless of the time bins chosen for the ancient samples. Preceding the isotopic decline, a relative stasis in average $\delta^{15}N$ values is supported by results from the islands of Oahu, Hawaii, and Maui. When the Modern time bin is excluded, there is no decline in $\delta^{15}N$ for Maui or Hawaii (Table S2). Similarly, before its extirpation around 600 B.P. (615 B.P., youngest date), there is no change in $\delta^{15}N$ of the Oahu population ($P = 1.00$). Overall, our data support a recent, species-wide shift in $\delta^{15}N$ that was unprecedented during the last 4,000 y.

We considered whether anthropogenic impact to $\delta^{15}N$ through a North Pacific–wide input of isotopically unique nitrogen could have influenced our results. However, atmospheric deposition of ^{15}N-depleted anthropogenic nitrogen to the ocean and a possible increase in nitrogen fixation together cannot explain even a 0.2‰ decrease in $\delta^{15}N$ values (see modeling in *SI Text S1*). Additionally, we find no evidence that Hawaiian petrel $\delta^{13}C$ or $\delta^{15}N$ values vary with the El Niño Southern Oscillation or longer term climatic perturbations (*Materials and Methods*) (15). Furthermore, because all modern island populations have lower average $\delta^{15}N$ values than all ancient populations, migration among islands cannot explain the $\delta^{15}N$ decline. This conclusion is supported by genetic analyses, which show that migration was very low among islands before human colonization and is currently low among extant populations (17, 18).

We considered whether declining population size in the Hawaiian petrel could be causally linked with the observed isotopic shift. However, the timing of $\delta^{15}N$ decline argues against this explanation. Our analysis identifies the isotopic shift occurring most likely within the past 100 y. While the population trend over the past century is not well documented, the majority of population
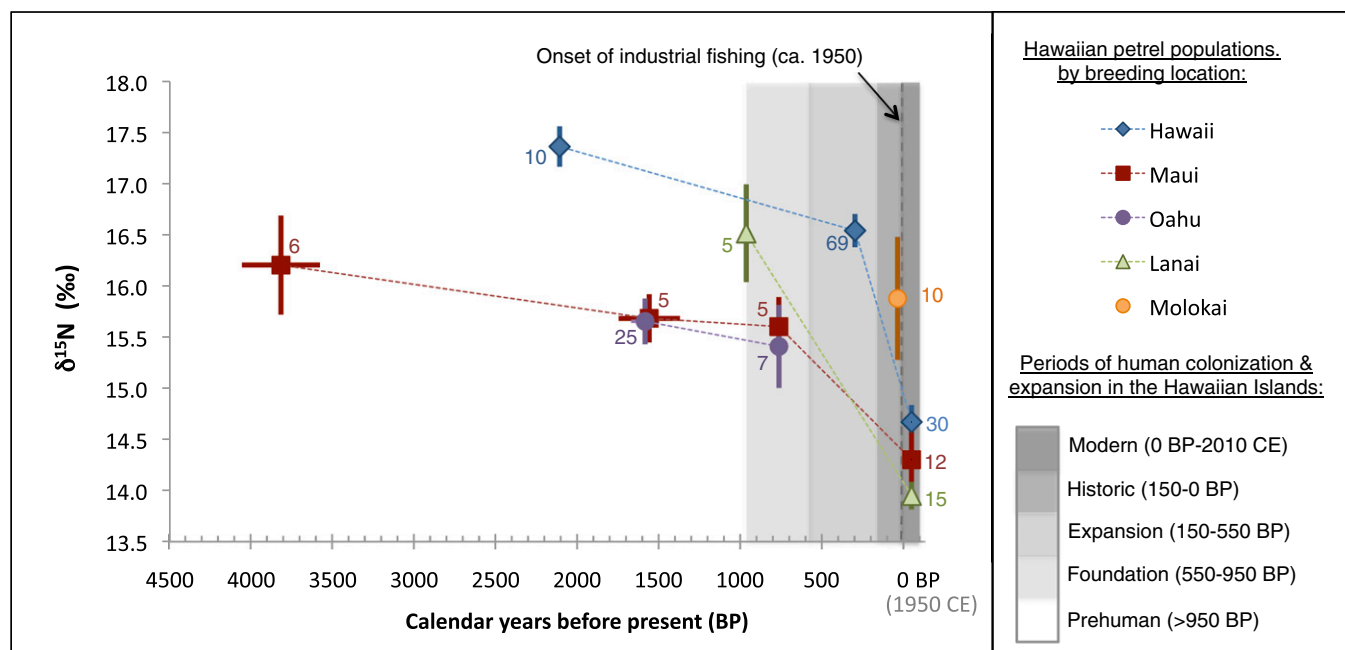
Fig. 3. $\delta^{15}N$ values of modern and radiocarbon-dated bone collagen for five Hawaiian petrel populations. The average age and isotopic composition of each time bin, ± SE, is plotted with sample size noted (see Fig. S1 for $\delta^{13}C$ results and Fig. S2 for confidence intervals of radiocarbon dates). Gray shading indicates time bins. Modern samples were unavailable from Oahu and Molokai due to population extirpation. Stippled lines connecting data points are for visualization purposes; isotopic shifts between time bins may have occurred nonlinearly. CE, Common Era.

decline in the Hawaiian petrel likely occurred before the 20th century, based on the bone record and on indigenous knowledge. Population decline due to human-induced causes (direct harvesting by people, habitat change, predation from introduced mammalian predators) is thought to have begun around 1,000 to 800 y ago, when people first arrived in the Hawaiian Islands, and to have continued during the prehistoric Foundation and Expansion periods (4, 26, 27). By around 600 y ago, according to our radiocarbon chronology, the extensive Hawaiian petrel population on the island of Oahu was extirpated. Based on our survey of paleontological bones, the species' breeding distribution on Maui, Molokai, and Hawaii also contracted dramatically during the Foundation and Expansion periods (*Materials and Methods*). In this regard, the Hawaiian petrel was no exception. Paleontological sites record the extinction of over half of the endemic species of Hawaiian birds and the extirpation of many other breeding seabird populations during these periods (28–30). Similar extirpations of procellariiform seabird colonies are recorded in the archaeological record on many other Pacific islands (31). Our study was designed in part to reveal whether prehistoric human-mediated seabird decline in the Pacific had a measureable effect on seabird foraging ecology, and our results do not support such an effect.

We also considered the possibility that breeding habitat is correlated with foraging behavior, such that the breeding range contraction in the Hawaiian petrel following human arrival and settlement (Fig. 1 and *Material and Methods*) led to an apparent shift in foraging. However, modern populations on Kauai and Lanai breed in similar habitats (densely vegetated, >1,000 cm rain per year, ≤1,000 m elevation) (25, 32), and the average $\delta^{15}N$ of their feathers is more disparate than any other two populations of Hawaiian petrels (Fig. 2*B*). Similarly, $\delta^{15}N$ values of feathers from Hawaii and Maui are distinct, although colonies on both islands exist in dry, sparsely vegetated environments above 2,000 m elevation (12, 25). Thus, breeding habitat does not appear to be a dominant control of $\delta^{15}N$ values.

We could not detect any fluctuations in $\delta^{13}C$ through time after correction for the depletion of ^{13}C in atmospheric CO_2 due to fossil fuel burning ([Fig. S1]; $P = 0.22$ for Lanai, $P \geq 0.99$ for all other within-island time bin comparisons). Because of the established, negative relationship between latitude and $\delta^{13}C$ in marine food webs (20–22), any shift in average petrel foraging location through time must have been largely constrained to longitudinal movement. If a change in foraging location accounted for the temporal shift in $\delta^{15}N$, all Hawaiian petrel populations must have dispersed, longitudinally, away from a region of the eastern tropical North Pacific characterized by high $\delta^{15}N$ (e.g., 4–10°N, 130–140°W; Fig. 2*A*) (23, 24). This explanation is unlikely because it requires several assumptions that are inconsistent with our knowledge of the Hawaiian petrel. First, all populations must have moved in the same direction, despite our observation that populations have distinct and in some cases seasonally dynamic foraging locations. Second, a shift away from a region of elevated $\delta^{15}N$ must have occurred alongside isotopic convergence of populations. This scenario is particularly unlikely as it would involve, before the isotopic shift, either (*i*) populations having relied to a greater extent on one particular area, while simultaneously showing stronger spatial segregation, isotopically, or (*ii*) populations of a single, opportunistic species, most of which are morphologically indistinguishable (25), having fed in a similar area in the past, but on vastly different prey.

Why then did $\delta^{15}N$ decline in our oceanic study species? Most likely, the isotopic shift reflects a species-wide decline in trophic level. Based on an estimated increase of 3‰ with each trophic level (33), our $\delta^{15}N$ data translate to a decline of one-half, four-fifths, and two-thirds of a trophic level for the populations on Maui, Lanai, and Hawaii, respectively. Studies of freshwater and near-shore marine ecosystems show that similar trophic declines

in generalist seabirds are associated with fishing pressure and declines in prey abundance (34–36). Consistent with this trend, $\delta^{15}N$ decline in the Hawaiian petrel was coincident with the onset of large-scale, industrial fishing in the oceanic Pacific, which could have affected petrel diet through several mechanisms. Many seabirds, including Hawaiian petrels, forage in association with schools of large predatory fish, such as tuna, that drive prey to the ocean surface. Fishery-induced loss of large predators (6, 7) could therefore have reduced feeding opportunities for the Hawaiian petrel or affected the abundance of their prey through a shift in predation rates and a potential trophic cascade, such as that observed in the Scotian Shelf following the collapse of cod populations (2, 37). Fisheries may have also altered Hawaiian petrel diet through the direct harvest or bycatch of petrel prey (e.g., flying fish, *Stenoteuthis oualaniensis*) (38). Regardless of the proximate cause, the recent timing of the species-wide shift in Hawaiian petrel $\delta^{15}N$ and the isotopic stasis preceding this shift strongly implicate anthropogenic alterations. Considering the links between fisheries and Hawaiian petrel foraging, including known impacts to large predatory fish populations, and in view of previous studies of fishery-associated trophic decline in seabirds, our record from the Hawaiian petrel provides evidence that the indirect effects of fishing on marine food webs extend beyond near-shore regions, reaching tropical and temperate oceanic waters.

Some predators may respond positively to fishery-mediated changes, such as seabirds that rely on fishery offal and discards (39) or midtrophic level fish that may benefit from declines in apex predator populations (6, 37). However, Hawaiian petrels are unlikely to use fishery subsidies (15), and the species that appear to have increased in abundance since the onset of industrial fishing in the Northeast Pacific do not include known Hawaiian petrel prey (6, 12, 37). Instead, our study shows that concurrent with the onset of industrialized fishing, the Hawaiian petrel underwent a species-wide shift in foraging habits that was seemingly unprecedented during the last four millennia. Further research is needed to understand the implications of trophic decline for population viability of this endangered species. Because the ratio of body mass between marine trophic levels is often greater than 100:1 (40, 41), it is possible that a 1/2–2/3 trophic level decline represents a reduction in the average body mass of petrel prey to 1/50–1/67 of its previous size ([SI Text S2]). Isotopic convergence of Hawaiian petrel populations, coincident with $\delta^{15}N$ decline, further suggests that trophic decline may have caused populations to become more comparable in their foraging habits, perhaps by limiting them to similar, lower trophic-level prey. Conservation efforts for most seabirds focus on breeding grounds where habitat loss and predation from introduced species are obvious hazards (42, 43). However, rapidly shifting or disappearing prey bases may be a hidden threat to Hawaiian petrels and other marine species. Indeed, given the evidence of trophic decline for multiple petrel populations with varied foraging habits, our results suggest a broad-scale shift in the composition of oceanic food webs in the Northeast Pacific.

Materials and Methods

Sample Acquisition, Feather Growth, and Subfossil Distribution. We sampled 83 primary 1 (P1; the innermost primary) feathers and 55 bones from Hawaiian petrel carcasses recovered between 1989 and 2009. We also sampled P1 feathers from two birds prepared as museum study skins in 1980 and 1995 and bones from 10 museum study skins prepared in 1914 (adults from the island of Molokai).

In hatch-year Hawaiian petrels, P1 and other flight feathers are formed during the late growth stages in the breeding season, from September to December (12, 15). As in other *Pterodroma*, adult Hawaiian petrels are presumed to begin primary molt, beginning with P1, during the non-breeding season, following cessation of nest attendance (November to December for breeders) (44, 45). Sample sizes for flight feathers are as follows: Hawaii adults (*n* = 14), Hawaii hatch-years (*n* = 7), Kauai adults (*n* = 13),

Kauai hatch-years (n = 12), Maui adults (n = 13), Maui hatch-years (n = 9), and Lanai adults (n = 17).

We sampled 132 subfossil bones from sites across four of the Hawaiian Islands (Fig. 1; see ref. 18 for distinction between archaeological and paleontological sites). The distribution of the paleontological sites helps to record the former breeding range of the Hawaiian petrel, which was more extensive than either the modern or historical range. The Hawaiian petrel was not recorded historically from Oahu, West Molokai, or the leeward slope of Haleakala Volcano on Maui (46). Its subfossil bones, however, are abundant and widespread on the extensive `Ewa Plain of southwest Oahu, to near sea level; they also occur near sea level in the dunes of West Molokai, and in lava caves of East Maui, documenting a former breeding range down slope as far as 808 m above sea level (asl) at Lua Lepo Cave (28, 29). On the island of Hawaii, active burrows have been recorded historically only from above 2,500 m asl on Mauna Kea and from above 1,800 m asl on Mauna Loa, although 19th-century interviews record indigenous knowledge of a wider prior breeding range, particularly in the saddle region between Mauna Loa and Mauna Kea (46). However, the species is very common and widespread in paleontological sites that extend past the known historic range, including areas in North Kona from the saddle region down to Kawaihai Bay, in the Puu Waawaa region of Hualalai Volcano, as well as in South Kona to near South Point.

Stable Isotope and Accelerator Mass Spectrometry Radiocarbon Methods. Before stable isotope analysis, feathers were washed in solvent (87:13 chloroform–methanol, v:v), rinsed with ultrapure distilled water (E-Pure, Barnstead), and dried at 25 °C in a vacuum oven. Stable isotope data were obtained from samples representative of the entire feather vanes (47).

Collagen was isolated and purified using a method modified from Stafford et al. (48). Bones were decalcified with quartz-distilled hydrochloric acid (0.2–0.5 M) and soaked in 0.05 M potassium hydroxide overnight to remove humate contaminants. The resulting collagen was gelatinized with 0.05 M hydrochloric acid (110 °C, 1–3 h), passed through a 0.45 μm Millipore HV filter, and lyophilized. One aliquot of gelatinized collagen was used for stable isotope analysis. For ancient samples, a second aliquot of gelatinized collagen was hydrolyzed in hydrochloric acid (6 M, 22 h) and passed through a column containing XAD-2 resin to remove fulvic acids. The resulting hydrolysate was dried, combusted to CO_2, and graphitized for Accelerator Mass Spectrometry (AMS) dating (W. M. Keck Carbon Cycle AMS laboratory, University of California, Irvine). Background contamination from ^{14}C-depleted and ^{14}C-enriched carbon during the preparation of each sample set was evaluated by dating hydrolyzed gelatin of known age: ^{14}C-dead whale (ca. 70,000 y B.P). and *Bison bison* (mean pooled radiocarbon age, 1,794 ± 5.8 y B.P., n = 9).

For 10 ancient samples, collagen was extracted at the Keck facility using techniques modified from Longin 1971, followed by ultrafiltration (49, 50). We demonstrated the comparability of dates obtained using XAD-2 purification versus Longin-ultrafiltration methods. First, we compared dates obtained from the *B. bison* sample (median probabilites of 1,740–1,820 y B.P., n = 10, by XAD purification; 1,750–1,785 y B.P., n = 2, for Longin-ultrafiltration). Second, we compared dates from Hawaiian petrel bones found in a short-term archaeological site, Fireplow Cave, Hawaii (median probabilities of 459–525 y B.P., n = 4, for XAD purification; 473–482 y B.P., n = 3, for Longin-ultrafiltration). In both cases, dates for the Longin-ultrafiltration methods fell within the range of those prepared using XAD purification.

We calibrated our conventional radiocarbon ages using the program CALIB 6.0 and applied a marine reservoir correction to account for incorporation of ^{14}C-depleted marine carbon. Specifically, we included a global model of the marine reservoir effect (Marine09 model), along with a regional correction, or ΔR, of 54 ± 20 y, calculated specifically for the Hawaiian petrel. We calculated our correction for the Hawaiian petrel by comparing radiocarbon dates on Hawaiian petrels and a terrestrial species (Hawaiian goose, *Branta sandvicensis*) in a short-term archaeological site, and also by obtaining radiocarbon dates on known-age museum specimens of the Hawaiian petrel collected in 1914–1917, before the age of atmospheric nuclear bomb testing. All radiocarbon dates referred to in the text are median probabilities, or the average of median probabilities from a group of samples. Similarly, median probability dates were used for all graphing and statistical analysis.

$\delta^{13}C$ and $\delta^{15}N$ values of gelatinized collagen (ca. 1.0 mg) were determined using an elemental analyzer (Eurovector) interfaced to an Isoprime mass spectrometer (Elementar). Stable isotope values are expressed in per mil (‰) as: $\delta X = ([R_{sample}/R_{standard}] - 1) \times 1,000$, where X is ^{13}C or ^{15}N, R is the corresponding ratio $^{13}C/^{12}C$ or $^{15}N/^{14}N$, and $R_{standard}$ is Vienna-Pee Dee Belemnite and air for $\delta^{13}C$ and $\delta^{15}N$, respectively. Precision was ≤0.2‰ for both $\delta^{13}C$ and $\delta^{15}N$.

We corrected for the Suess Effect using an ice-core–based estimate of the rate of $\delta^{13}C$ decrease in the atmosphere: 0.22‰ per decade since 1960, and 0.05‰ per decade between 1860 and 1960 (51, 52). All stable isotope and radiocarbon data from subfossil bones can be found in Table S3. Stable isotope data from modern and historic bones and feathers are in Table S4.

Temporal and Statistical Analysis. Isotope data from gelatinized collagen were binned based on archaeological and historical time periods marking the growth and development of the human population of the Hawaiian Islands, plus one bin covering the modern period of industrial fishing. Based on Hawaiian archaeology and history, the following time bins were used: the Prehuman period (before human colonization; <1000 CE or >950 y B.P.), the Foundation period (time of Polynesian colonization, with small human population size; 1000–1400 CE; 550–950 y B.P.), the Expansion Period (characterized by increasing human population size; 1400–1800 CE; 150–550 y B.P.), the Historic Period (including the period of European colonization and whaling; 1800–1950 CE; 0–150 y B.P.), and the Modern period (a time of industrialized fishing in the North Pacific; 1950–2010 CE) (4, 6, 53). We subdivided the Prehuman time bin for the island of Maui in half along a natural gap in the data of >850 y, due to the exceptionally long period of ca. 3,500 y covered by those samples. We combined all ancient samples (>100 y old) from the island of Lanai into one time bin, due to their relatively narrow range of dates (899–1,088 y B.P.) and our small sample size (n = 5).

The effects of island population and time on collagen isotope values were evaluated through multiple ANOVA models. For $\delta^{15}N$ only (where both population and time had significant effects), Tukey HSD post hoc tests were used to make all possible pair-wise comparisons between population–time bin groups. ANOVA and Tukey HSD tests were similarly used to evaluate isotopic variation among modern feathers. Normal quantile–quantile plots and Levene's tests were used to check assumptions of normality and homogeneity of variance. All statistical tests were conducted using R statistical software (version 2.12.1, R Foundation for Statistical Computing, 2010).

Age Classification for Bones. Among subfossil bones in our ancient chronologies, six were identified as hatch-year birds (<1 y in age) based on osteological evidence of incomplete bone formation (using indications such as open sutures, spongy texture, and the presence of small pores and striations; SI Text S3 and Fig. S3): one from Oahu, three from Lanai, and two from Hawaii. For the island of Maui, all modern and ancient hatch-year bones were excluded from analysis due to the isotopic disparities observed between age classes in the modern population for both feather and bone (t test comparing six hatch-year and 10 adult bones: P = 0.021 for $\delta^{15}N$ and P = 0.018 for $\delta^{13}C$). We retained hatch-year petrels in our chronology for the island of Hawaii, because no isotopic disparity was observed between age classes for either feathers or bones in the modern population from this island (t test comparing eight hatch-year and 18 adult bones: P = 0.862 for $\delta^{15}N$ and P = 0.690 for $\delta^{13}C$), and because the average $\delta^{15}N$ value for the known hatch-year birds in the ancient chronology was the same as the average for all ancient Hawaii birds (16.6‰). While hatch-year birds were included in our ancient sample from Lanai, the modern sample from this island consists entirely of adults. For Lanai, the three ancient hatch-years have lower $\delta^{15}N$ values than the ancient adults, as we would expect based on the foraging pattern of breeding Lanai adults, which appears to be similar to that of Maui birds (13, 54). The inclusion of hatch-year petrels in the Lanai chronology will tend to lower the average $\delta^{15}N$ value for our ancient Lanai time bin, perhaps causing us to underestimate any $\delta^{15}N$ decline through time.

Effects of Climate on Hawaiian Petrel $\delta^{15}N$ Values. We used a measure of El Niño Southern Oscillation (ENSO), the Southern Oscillation Index (SOI), to evaluate potential impacts of climatic variation on $\delta^{15}N$ of modern Hawaiian petrel flight feathers. SOI values, standardized according to the methods of Trenberth 1984 (www.cgd.ucar.edu/cas/catalog/climind/soi.html) (55), were averaged over the months surrounding flight feather growth (September–December for hatch-year birds; November–March for adults, with SOI averages offset by 1 mo for all Maui petrels to account for their earlier breeding cycle; SOI values used in statistical analyses can be found in Table S4). We used an analysis of covariance (ANCOVA) to test for an effect of SOI while accounting for the variance associated with age class (adult vs. hatch-year) and population. Based on data from all of the flight feathers where year of collection was known (n = 82; Table S4), SOI had a statistically insignificant effect on $\delta^{15}N$ values (t value = 0.055, P = 0.9559). Additionally, we compared $\delta^{15}N$ values from the most data-rich El Niño event (Fall/Winter of 2006) and La Niña event (Fall/Winter of 2007) for petrels nesting on the islands of Lanai and Hawaii (all data combined, as the $\delta^{15}N$ values of these age

groups and populations were not significantly different). Because there was unequal variance in $\delta^{15}N$ among years (F statistic = 0.0039), we performed a Welch t test, which showed no significant difference in $\delta^{15}N$ between the El Niño and La Niña years ($t = -0.6282$, $P = 0.599$, $n = 18$, df = 6.928).

We also did not detect a significant difference in average isotope values between our Prehuman time bins (4,409–955 B.P.) and Foundation time bins (555–914 B.P.) (Fig. 2, Table S1), a time span that encompassed considerable climatic variation around the Pacific basin (e.g., Medieval Warm Period vs. cooling at ca. 1,500 B.P.) (56, 57).

1. Jackson JBC, et al. (2001) Historical overfishing and the recent collapse of coastal ecosystems. *Science* 293(5530):629–638.
2. Frank KT, Petrie B, Choi JS, Leggett WC (2005) Trophic cascades in a formerly cod-dominated ecosystem. *Science* 308(5728):1621–1623.
3. Rick TC, Erlandson JM (2008) *Human Impacts on Ancient Marine Ecosystmes: A Global Perspective* (Univ of California, Berkeley).
4. Wilmshurst JM, Hunt TL, Lipo CP, Anderson AJ (2011) High-precision radiocarbon dating shows recent and rapid initial human colonization of East Polynesia. *Proc Natl Acad Sci USA* 108(5):1815–1820.
5. Kirch PV (1985) *Feathered Gods and Fishhooks: An Introduction to Hawaiian Archaeology and Prehistory* (Univ of Hawaii, Honolulu).
6. Ward P, Myers RA (2005) Shifts in open-ocean fish communities coinciding with the commencement of commercial fishing. *Ecology* 86(4):835–847.
7. Myers RA, Worm B (2003) Rapid worldwide depletion of predatory fish communities. *Nature* 423(6937):280–283.
8. Pauly D, Christensen V, Dalsgaard J, Froese R, Torres F, Jr. (1998) Fishing down marine food webs. *Science* 279(5352):860–863.
9. Cairns DK (1987) Seabirds as indicators of marine food supplies. *Biol Oceanogr* 5:261–271.
10. Piatt I, Sydeman W (2007) Seabirds as indicators of marine ecosystems. *Mar Ecol Prog Ser* 352:199–204.
11. Ricklefs RE, Duffy D, Coulter M (1984) Weight gain of Blue-footed booby chicks: An indicator of marine resources. *Nordic Scandinavica* 15(3):162–166.
12. Simons TR (1985) Biology and behavior of the endangered Hawaiian Dark-rumped Petrel. *Condor* 87(2):229–245.
13. Adams J, Flora S (2009) Correlating seabird movements with ocean winds: Linking satellite telemetry with ocean scatterometry. *Mar Biol* 157(4):915–929.
14. Spear LB, et al. (1995) Population size and factors affecting at-sea distributions of four endangered procellariids in the tropical Pacific. *The Condor* 97(3):613–638.
15. Wiley AE, et al. (2012) Foraging segregation and genetic divergence between geographically proximate colonies of a highly mobile seabird. *Oecologia* 168(1):119–130.
16. Deniro MJ (1985) Postmortem preservation and alteration of in vivo bone collagen isotope ratios in relation to palaeodietary reconstruction. *Nature* 317(6040):806–809.
17. Welch AJ, et al. (2012) Population divergence and gene flow in an endangered and highly mobile seabird. *Heredity (Edinb)* 109(1):19–28.
18. Welch AJ, et al. (2012) Ancient DNA reveals genetic stability despite demographic decline: 3,000 years of population history in the endemic Hawaiian petrel. *Mol Biol Evol* 29(12):3729–3740.
19. Rucklidge GJ, Milne G, McGaw BA, Milne E, Robins SP (1992) Turnover rates of different collagen types measured by isotope ratio mass spectrometry. *Biochim Biophys Acta* 1156(1):57–61.
20. Goericke R, Fry B (1994) Variation of marine plankton $\delta^{13}C$ with latitude, temperature, and dissolved CO_2 in the world ocean. *Global Biogeochem Cycles* 8(1):85–90.
21. MacKenzie KM, et al. (2011) Locations of marine animals revealed by carbon isotopes. *Scientific Reports* 1:1–21.
22. Takai N, et al. (2000) Geographical variations in carbon and nitrogen stable isotope ratios in squid. *J Mar Biol* 80(4):675–684.
23. Altabet MA, Francois R (1994) Sedimentary nitrogen isotopic ratio as a recorder for surface ocean nitrate utilization. *Global Biogeochem Cycles* 8(1):103–116.
24. Graham BS, Koch PL, Newsome SD, McMahon KW, Aurioles D (2010) Using isoscapes to trace the movements and foraging behavior of top predators in oceanic ecosystems. *Isoscapes: Understanding Movement, Pattern and Process on Earth Through Isotope Mapping*, eds West J, Bowen GJ, Dawson TE, Tu KP (Springer, New York), pp 299–318.
25. Judge S (2011) *Interisland Comparison of Behavioral Traits and Morphology of the Endangered Hawaiian Petrel: Evidence for Character Differentiation* (University of Hawai'i at Hilo, Hilo, HI).
26. James HF, et al. (1987) Radiocarbon dates on bones of extinct birds from Hawaii. *Proc Natl Acad Sci USA* 84(8):2350–2354.
27. James HF (1995) Prehistoric extinctions and ecological changes on oceanic islands. *Ecological Studies* 115:88–102.
28. Olson SL, James HF (1982) Fossil birds from the Hawaiian islands: Evidence for wholesale extinction by man before Western contact. *Science* 217(4560):633–635.
29. Olson SL, James HF (1991) Descriptions of thirty-two new species of birds from the Hawaiian Islands: Part 1. Non-Passeriformes. *Ornithological Monographs* 45:1–88.
30. James HF, Olson SL (1991) Descriptions of thirty-two new species of birds from the Hawaiian Islands: Part 2. Passeriformes. *Ornithological Monographs* 46:1–88.
31. Steadman DW (1996) *Extinction and Biogeography of Tropical Pacific Birds* (Univ of Chicago, Chicago).
32. Ainley DG, Podolsky R, Deforest L, Spencer G (1997) New insights into the status of the Hawaiian Petrel on Kauai. *Colon Waterbirds* 20(1):24–30.
33. Michener RH, Schell DM (1994) Stable Isotope Ratios as Tracers in Marine Aquatic Food Webs. *Stable Isotopes in Ecology and Environmental Science*, eds Lajtha K, Michener R (Blackwell, Oxford), pp 138–157.
34. Becker BH, Beissinger SR (2006) Centennial decline in the trophic level of an endangered seabird after fisheries decline. *Conserv Biol* 20(2):470–479.
35. Farmer RG, Leonard ML (2011) Long-term feeding ecology of Great Black-backed Gulls (Larus marinus) in the northwest Atlantic: 110 years of feather isotope data. *Can J Zool* 89(2):123–133.
36. Hebert CE, et al. (2008) Restoring piscivorous fish populations in the Laurentian Great Lakes causes seabird dietary change. *Ecology* 89(4):891–897.
37. Polovina JJ, Abecassis M, Howell EA, Woodworth P (2009) Increases in the relative abundance of mid-trophic level fishes concurrent with declines in apex predators in the subtropical North Pacific, 1996-2006. *Fish Bull* 107(4):523–531.
38. FAO Fisheries and Aquaculture Department, Statistics and Information Service (2011) *FishStatJ: Universal Software for Fishery Statistical Time Series*.
39. Garthe S, Camphuysen CJ, Furness RW (1996) Amounts of discards by commercial fisheries and their significance as food for seabirds in the North Sea. *Mar Ecol Prog Ser* 136:1–11.
40. Brose U, et al. (2006) Consumer-resource body-size relationships in natural food webs. *Ecology* 87(10):2411–2417.
41. Jennings S, Warr KJ, Mackinson S (2002) Use of size-based production and stable isotope analyses to predict trophic transfer efficiencies and predator-prey body mass ratios in food webs. *Mar Ecol Prog Ser* 240:11–20.
42. Taylor RH, Kaiser GW, Drever MC (2000) Eradication of Norway rats for recovery of seabird habitat on Langara Island, British Columbia. *Restor Ecol* 8(2):151–160.
43. Nogales M, Mart A, Tershy BR, Donlan CJ, Veitch D (2004) A review of feral cat eradication on islands. *Conserv Biol* 18(2):310–319.
44. Pyle P (2008) Molt and age determination in Procellariiformes. *Identification Guide to North American Birds, Part 2* (Slate Creek Press, Point Reyes Station, CA), pp 248–260.
45. Warham J (1996) *The Behaviour, Population Biology and Physiology of the Petrels* (Academic, London).
46. Banko WE (1980) *History of Endemic Hawaiian Birds: Population Histories, Species Accounts: Sea birds: Hawaiian Dark-Rumped Petrel*, ed Smith CW (Univ of Hawaii at Manoa; Western Region, National Park Service, Honolulu, HI).
47. Wiley AE, Ostrom PH, Stricker CA, James HF, Gandhi H (2010) Isotopic characterization of flight feathers in two pelagic seabirds: Sampling strategies for ecological studies. *Condor* 112(2):337–346.
48. Stafford TW, Brendel K, Duhamel RC (1988) Radiocarbon, 13C and 15N analysis of fossil bone: Removal of humates with XAD-2 resin. *Geochimica et Chosmochimica Acta* 52(9):2257–2267.
49. Longin R (1971) New method of collagen extraction for radiocarbon dating. *Nature* 230(5291):241–242.
50. Brown TA, Nelson DE, Vogel JS, Southon JR (1988) Improved collagen extraction by modified Longin method. *Radiocarbon* 30(2):171–177.
51. Francey RJ, et al. (1999) A 1000-year high precision record of $\delta^{13}C$ in atmospheric CO_2. *Tellus B Chem Phys Meterol* 51(2):170–193.
52. Chamberlain CP, et al. (2005) Pleistocene to recent dietary shifts in California condors. *Proc Natl Acad Sci USA* 102(46):16707–16711.
53. Kirch PV (1990) The evolution of sociopolitical complexity in prehistoric Hawaii: An assessment of the archaeological evidence. *J World Prehist* 4(3):311–345.
54. VanZandt MLA (2012) Distribution and Habitat Selection of the Endangered Hawaiian Petrel (*Pterodroma sandwichensis*), from the Island of Lana'i. Thesis (University of Hawai'i, Hilo, HI).
55. Trenberth KE (1984) Signal versus noise in the Southern Oscillation. *Weather Review* 112(2):326–332.
56. Grove JM (2004) *Little Ice Ages: Ancient and Modern* (Routledge, London), 2nd Edition.
57. Nunn P (2007) *Climate, Environment and Society in the Pacific During the Last Millennium*, ed Nunn PD (Elsevier, Amsterdam).
58. Athens JS, Kaschko MW, James HF (1991) Prehistoric bird hunters: High altitude resource exploitation on Hawai`i Island. *Bishop Museum Occasional Papers* 31:63–84.

ECOLOGY

ENVIRONMENTAL SCIENCES

Supporting Information

Wiley et al. 10.1073/pnas.1300213110

SI Text 1

Estimating the Impact of Anthropogenic Atmospheric Nitrogen on Nitrogen Isotope Values. We estimated the expected change in the $\delta^{15}N$ of inorganic nitrogen from the input of anthropogenic atmospheric nitrogen (AAN) to ocean food webs. The estimate was obtained by taking the difference in $\delta^{15}N$ between average marine inorganic nitrogen (predominantly nitrate) and nitrogen derived from a mixture of average marine nitrate and AAN. Inorganic nitrogen is used by phytoplankton and subsequently transferred to consumers via the food web. Thus, inorganic nitrogen influences the $\delta^{15}N$ of predators such as the Hawaiian petrel.

The $\delta^{15}N$ of average marine nitrate is 5‰ (1). The $\delta^{15}N$ of the mixture of average marine nitrate and AAN estimated using the mass balance model below is 4.97‰:

$$\delta^{15}N_x = F_a * \delta^{15}N_a + F_m * \delta^{15}N_m,$$

where $\delta^{15}N_x$ is the nitrogen isotope value of a mixture of marine nitrate and AAN; F_a is the fraction of global production that is supplied by AAN [global ocean productivity resulting from AAN/global ocean productivity = 0.31 PgC year^{-1}/50 PgC year^{-1} = 0.006 (2)]; $\delta^{15}N_a$ is the nitrogen isotope value of AAN [AAN is inorganic nitrogen derived from the Haber–Bosch process, which has a value of ca. 0 ‰ (3)]; F^{15}_m is the fraction of global production that is supplied by marine nitrate, $1 - F_a = 0.994$; and δN_m is the nitrogen isotope value of average marine nitrate, 5‰ (1).

The maximum change in $\delta^{15}N$ resulting from the introduction of AAN is therefore:

$$\delta^{15}N_m - \delta^{15}N_x = 5‰ - 4.97‰ = 0.03‰.$$

Estimating the Impact of Enhanced Supply of Biologically Fixed Nitrogen on Nitrogen Isotope Values. Approximately 1% of global primary production is attributed to biological nitrogen fixation (BNF; the conversion of N_2 gas to ammonium) (2). Using this value, we estimate the degree to which BNF could change the $\delta^{15}N$ of inorganic nitrogen by taking the difference between the isotope value of average marine inorganic nitrogen (predominantly nitrate) to that derived from a mixture of average marine nitrate and inorganic BNF-derived nitrogen. Inorganic nitrogen is taken up by phytoplankton and transferred to consumers higher in the food web. Thus, widespread changes in the rate of BNF through time have the potential to impact our record from the Hawaiian petrel. Because our model assumes that BNF did not occur in the past, it overestimates the influence of BNF on $\delta^{15}N$.

The average $\delta^{15}N$ of marine nitrogen is estimated to be 5‰ (1). The $\delta^{15}N$ of the mixture of average marine nitrate and BNF estimated using the mass balance model below is 4.95‰:

$$\delta^{15}N_y = F_f * \delta^{15}N_f + F_m * \delta^{15}N_m,$$

where $\delta^{15}N_y$ is the nitrogen isotope value of a mixture of marine nitrate and BNF-derived nitrogen; F_f is the fraction of global production that is supplied by BNF—global ocean productivity resulting from BNF/global ocean productivity = 0.57 PgC year^{-1}/50 PgC year^{-1} = 0.01 (2); $\delta^{15}N_f$ is the nitrogen isotope value of BNF-derived nitrogen—ammonium derived from BNF has a value of ca. 0‰ (3); F_m is the fraction of global production that is supplied by marine nitrate, $1 - F_a = 0.99$; and $\delta^{15}N_m$ is the nitrogen isotope value of average marine nitrate = 5‰ (1).

The maximum change in $\delta^{15}N$ resulting from the introduction of BNF is therefore:

$$\delta^{15}N_m - \delta^{15}N_y = 5‰ - 4.95‰ = 0.05‰.$$

We also estimated the influence of BNF in the north Pacific Subtropical Gyre (station ALOHA, A Long-Term Oligotrophic Habitat Assessment; 22° 45′ N, 158° 00′ W) using the approach above. We incorporate an estimate of 6.5‰ for $\delta^{15}N_m$ and an estimate of 2% for the contribution of BNF to production at station ALOHA (4, 5). The contribution of BNF to production is the average estimate of nitrogen fixation (41 mmol m^{-2}·year^{-1}) divided by the particulate nitrogen flux at station ALOHA (2,044 mmol N m^{-2}·yr^{-1}). The maximum change in $\delta^{15}N$ resulting from the introduction of BNF is therefore:

$$\delta^{15}N_m - \delta^{15}N_y = 6.5‰ - 6.37‰ = 0.13‰.$$

SI Text 2

Hawaiian Petrel Prey Size. The $\delta^{15}N$ composition of many oceanic fish and squid, including known Hawaiian petrel prey, increases with body mass (6, 7). The temporal decline in $\delta^{15}N$ values observed for Hawaiian petrels could therefore result from a decline in the average size of their prey. Given the diverse diet and broad range of the Hawaiian petrel, its species-wide $\delta^{15}N$ decline is likely driven by changes in multiple prey species. However, we can use data from a single species to demonstrate the approximate decrease in prey size that may have driven a shift in petrel trophic level.

We have identified several *Sthenotheuthis oualaniensis* in modern Hawaiian petrel regurgitations. $\delta^{15}N$ values of this species in the Northeast Pacific vary between 4 and 10‰, depending on size (7). To account for the 1.8‰ decline in Hawaiian petrel $\delta^{15}N$ values observed for the population on Hawaii, the average mantle length of *S. oualaniensis* would have decreased from 224 to 77 mm (77 mm is the average mantle length observed in modern petrel regurgitations). Hawaiian petrels take prey across this range: among seven measurable squid from Hawaiian petrel regurgitations, mantle length varied from 45 to 233 mm (in *S. oualaniensis* and *Taonius pavo*, respectively), with projected masses of 5–44 g. This order of magnitude variation in prey mass demonstrates the Hawaiian petrel's opportunistic foraging habits and the potential for large shifts in the size of exploited prey. Through size-selective harvesting of marine organisms, fishing can decrease the average size and change the age structure of exploited species and marine communities (8). Fishing is therefore capable of causing a decrease in the size of prey available for Hawaiian petrel consumption (e.g., through the use of size-selective fishing gear). Reductions in the size class of petrel prey may also result from the removal of large predatory fish and resultant changes to oceanic food web structure.

SI Text 3

Distinguishing Skeletons of Adult Hawaiian Petrels from Adult-Sized Hatch-Year Birds. Bones of hatch-year Hawaiian petrels are distinctly smaller and more porous than bones of adult birds, except in the case of hatch-years that died close to, or after, the time of fledging. The bones of fledglings are comparable in size to adults, but still show signs of active or recent growth. In most cases, adult-sized hatch-year birds are readily distinguishable from adult birds by examining the bones with a dissecting microscope (2–6×). In the hatch-year birds, sutures are partially open between certain

compound bones (e.g., lacrimal incompletely fused to the neurocranium, suture between nasal bones extending farther anterior than in adults); bony surfaces, especially of the major wing bones, the tarsometatarsus, and the maxilla, are pitted and striated in places (Fig. S3); muscle impressions and growth zones may have a spongy texture; and there is a higher density of small nutrient foramina at the articular ends of some long bones. As the bird matures further, the boney surfaces become smoother and less vascularized. Among the most persistent signatures of a hatch-year bird are the higher density of small nutrient foramina on the proximal tarsometatarsus, the incomplete

fusion of the lacrimals, and the spongy or rugose texture of fossa musculus brachialis on the humerus and impressio brachialis on the ulna. Some bones, such as the coracoid and femur, mature quickly and are not reliable for distinguishing older hatch-year birds from adults. These observations are based on the series of skeletons of Hawaiian petrel and Newell's shearwater in the skeleton collection of the National Museum of Natural History, Division of Birds, which includes numerous specimens of hatch-year birds that had already fledged at the time of death.

1. Sigman DM, Altabet MA, McCorkle DC, Francois R, Fischer G (2000) The $\delta^{15}N$ of nitrate in the Southern Ocean: Nitrogen cycling and circulation in the ocean interior. *J Geophys Res* 105(C8):19599–19614.
2. Duce RA, et al. (2008) Impacts of atmospheric anthropogenic nitrogen on the open ocean. *Science* 320(5878):893–897.
3. Macko SA, Ostrom NE (1994) Pollution studies using stable isotopes. *Stable Isotopes in Ecology and Environmental Science*, eds Lajtha K, Michener RH (Blackwell, Boston), pp 45–62.
4. Karl D, et al. (1997) The role of nitrogen fixation in biogeochemical cycling in the subtropical North Pacific Ocean. *Nature* 388(6643):533–538.
5. Dore JE, Brum JR, Tupas LM, Karl DM (2002) Seasonal and interannual variability in sources of nitrogen supporting export in the oligotrophic subtropical North Pacific Ocean. *Limnol Oceanogr* 47(6):1595–1605.
6. Ruiz-Cooley RI, Villa EC, Gould WR (2010) Ontogenetic variation of $\delta^{13}C$ and $\delta^{15}N$ recorded in the gladius of the jumbo squid Dosidicus gigas: Geographic differences. *Mar Ecol Prog Ser* 399:187–198.
7. Parry M (2007) Trophic variation with length in two ommastrephid squids, Ommastrephes bartramii and Sthenoteuthis oualaniensis. *Mar Biol* 153(3):249–256.
8. Stergiou KI (2002) Overfishing, tropicalization of fish stocks, uncertainty and ecosystem management: Resharpening Ockham's razor. *Fish Res* 55:1–9.

Fig. S1. Suess-corrected $\delta^{13}C$ values of modern and radiocarbon-dated bone collagen for five Hawaiian petrel populations. The average age and isotopic composition of each time bin, ±SE, is plotted with sample size noted. Gray shading indicates time bins. Modern samples were unavailable from Oahu and Molokai due to population extirpation. Stippled lines connecting data points are for visualization purposes; isotopic shifts between time bins may have occurred nonlinearly.

Fig. S2. The 95% confidence interval of 133 calibrated radiocarbon dates used in the present study (median ages marked by diamonds within confidence intervals).

Fig. S3. Shafts of seabird humeri, illustrating one example of the observed differences in bone surface morphology between adult-sized hatch-year birds, and adults. (*A*) USNM 556797, a hatch-year Newell's shearwater; (*B*) USNM 639525, an adult Newell's shearwater; (*C*) MDS2005HY, a subfossil hatch-year Hawaiian petrel; and (*D*) MDS2005AD, a subfossil adult Hawaiian petrel. The hatch-year bones show pits and striations indicative of vascularization, whereas the adult bones show a smooth surface. Pictures taken with a Zeiss Axiocam attached to a Zeiss Stereo Discovery V12, and prepared with Zeiss AxioVision software to increase the depth of field.

Table S1. Tukey honestly significant difference post hoc comparisons for δ^{15}N (above diagonal) and δ^{13}C values (below diagonal) of Hawaiian petrel flight feathers

Island-age	Hawaii A	Hawaii HY	Lanai A	Maui A	Maui HY	Kauai A	Kauai HY
Hawaii A	—	1.000	0.999	0.071	<0.001*	<0.001*	<0.001*
Hawaii HY	0.992	—	0.999	0.272	<0.001*	<0.001*	<0.001*
Lanai A	0.999	0.910	—	0.009*	<0.001*	<0.001*	<0.001*
Maui A	0.999	0.999	1.000	—	0.006*	0.247	<0.001*
Maui HY	<0.001*	<0.001*	<0.001*	<0.001*	—	0.716	1.000
Kauai A	0.999	0.910	1.000	<0.001*	0.844	—	0.449
Kauai HY	<0.001*	<0.001*	<0.001*	<0.001*	0.844	<0.001*	—

P values are shown. Age classes are abbreviated as A (adult) and HY (hatch-year bird).
*Statistically significant difference ($\alpha = 0.05$).

Table S2. Tukey HSD post hoc comparisons for δ^{15}N values of Hawaiian petrel collagen

Island-Bin	Hawaii 3	Hawaii 4	Maui 1	Maui 4	Maui 5	Maui 6	Oahu 4	Oahu 5	Lanai 1	Lanai 4	Molokai 2
Hawaii 1	<0.01*	<0.01*	0.993	0.854	0.684	0.064	0.887	0.041	0.520	0.021*	0.090
Hawaii 3	—	0.441	<0.01*	0.661	0.843	1.000	0.219	0.020	<0.01*	1.000	0.768
Hawaii 4		—	<0.01*	0.037*	0.077	0.427	<0.01*	<0.01*	<0.01*	0.882	0.072
Maui 1			—	0.345	0.202	<0.01*	0.359	<0.01*	0.998	<0.01*	0.024*
Maui 4				—	1.00	0.990	1.000	1.000	0.065	0.893	1.000
Maui 5					—	0.999	1.000	1.000	0.028*	0.961	1.000
Maui 6						—	0.929	0.977	<0.01*	1.00	1.000
Oahu 4							—	1.000	0.050*	0.686	0.999
Oahu 5								—	<0.01*	0.769	1.000
Lanai 1									—	<0.01*	<0.01*
Lanai 4										—	0.993

P values are shown. Numbers refer to time bins, as defined in *Materials and Methods*, with 1 indicating the Modern time bin, or Modern Period, and moving backward in time, with 5 indicating the earliest Prehuman time bin.
*Statistically significant difference ($\alpha = 0.05$).

Table S3. Radiocarbon data, isotope values, and museum specimen information for ancient Hawaiian petrel bone samples

Sample ID	Museum	Catalog	Island	Location	δ¹⁵N (‰)	δ¹³C (‰)	Median age (B.P.)	¹⁴C age (B.P.)
NA	BPBM	1992.166.1	Hawaii	Puu Waawaa	17.3	−13.84	3,228	3,410 ± 25
BBM1992.166.2	BPBM	1992.166.2	Hawaii	Puu Waawaa	17.08	−14.02	1,777	2,235 ± 25
NA	BPBM	X157438	Hawaii	Puuanahulu	17.8	−13.53	278	685 ± 20
NA	BPBM	X150206	Maui	Haleakala Crater	14.87	−13.09	651	1,140 ± 15
RCF-05–01	USNM	NA	Hawaii	Fireplow Cave	14.9	−13.4	428	835 ± 25
HFJ-05–4a	USNM	NA	Hawaii	Pohakuloa 10649	16.69	−13.06	382	795 ± 15
HFJ-05–8a	USNM	NA	Hawaii	Waikulukulu Cave	17.5	−13.5	479	900 ± 20
HFJ-06–17	USNM	NA	Hawaii	Fireplow Cave	15.0	−14.1	422	830 ± 25
HFJ-06–21	USNM	NA	Hawaii	Fireplow Cave	15.1	−14.1	437	845 ± 25
RCF-05–03	USNM	NA	Hawaii	Palisades Cave	16.24	−13.35	294	705 ± 15
RCF-05–04	USNM	NA	Hawaii	Fireplow Cave	15.76	−13.59	413	820 ± 20
HFJ-05–3a	USNM	NA	Hawaii	Pohakuloa 10649	15.2	−14.1	302	710 ± 25
HFJ-05–5a	USNM	NA	Maui	Kiakeana Cave	16.01	−12.67	1,144	1,635 ± 20
HFJ-05–7a	USNM	NA	Maui	Puu Makua Cave	15.4	−13.9	1,527	2,025 ± 25
HFJ-06–35R	USNM	NA	Maui	Kiakeana Cave	14.23	−12.85	769	1,285 ± 20
HFJ-06–36	USNM	NA	Maui	Kahawaihapapa Cave	16.4	−13.1	3,435	3,605 ± 25
HFJ-06–26	USNM	391137	Oahu	50–80-12–2706-22B	14.48	−13.76	699	1,210 ± 20
HFJ-06–27	USNM	391137	Oahu	50–80-12–2706-22B	16.24	−12.91	644	1,130 ± 15
HFJ-06–31	USNM	392735	Oahu	Barber's Point 9670-P1	14.0	−14.5	1,546	2,040 ± 20
HFJ-06–33	USNM	391317	Oahu	Barber's Point 9670-P1	16.6	−12.5	1,702	2,170 ± 20
HFJ-06–01	USNM	391422	Oahu	Barber's Point 9670-P1	14.18	−13.85	615	1,095 ± 20
SC 01	NA	NA	Hawaii	Shangri-la Cave	16.49	−13.2	383	795 ± 15
SC 03	NA	NA	Hawaii	Shangri-la Cave	17.52	−12.34	234	640 ± 15
SC 04	NA	NA	Hawaii	Shangri-la Cave	17.08	−12.73	352	760 ± 15
SC 05	NA	NA	Hawaii	Shangri-la Cave	17.24	−12.45	230	640 ± 20
SC 06	NA	NA	Hawaii	Shangri-la Cave	18.04	−12.49	262	665 ± 20
SC 07	NA	NA	Hawaii	Shangri-la Cave	16.86	−12.78	270	675 ± 20
SC 08	NA	NA	Hawaii	Shangri-la Cave	17.24	−13.39	1,632	2,115 ± 20
AM 03	NA	NA	Hawaii	Ambigua Cave	15.68	−13.36	293	705 ± 15
AM 04	NA	NA	Hawaii	Ambigua Cave	17.91	−12.65	233	640 ± 15
AM 05	NA	NA	Hawaii	Ambigua Cave	16.31	−13.73	186	600 ± 15
AM 06	NA	NA	Hawaii	Ambigua Cave	17.48	−13.38	214	630 ± 20
AM 07	NA	NA	Hawaii	Ambigua Cave	16.18	−13.7	239	645 ± 20
AM 08	NA	NA	Hawaii	Ambigua Cave	15.51	−13.39	246	650 ± 20
AM 09	NA	NA	Hawaii	Ambigua Cave	16.6	−13.12	348	755 ± 20
AM 10	NA	NA	Hawaii	Ambigua Cave	17.75	−13.22	246	650 ± 20
AM 11	NA	NA	Hawaii	Ambigua Cave	17.16	−13.02	234	640 ± 15
AM 12	NA	NA	Hawaii	Ambigua Cave	18.37	−13.11	254	655 ± 15
AM 13	NA	NA	Hawaii	Ambigua Cave	16.43	−13.54	210	625 ± 15
PC 86	NA	NA	Hawaii	Petrel Cave	15.58	−13.99	222	635 ± 20
PC 87	NA	NA	Hawaii	Petrel Cave	16.16	−13.17	243	650 ± 25
PC 88	NA	NA	Hawaii	Petrel Cave	17.45	−14.06	1,654	2,135 ± 15
PC 90	NA	NA	Hawaii	Petrel Cave	15.3	−14.27	263	665 ± 15
PC 91	NA	NA	Hawaii	Petrel Cave	14.49	−13.68	246	650 ± 20
PC 92	NA	NA	Hawaii	Petrel Cave	17.31	−13.26	203	620 ± 20
PC 93	NA	NA	Hawaii	Petrel Cave	16.08	−13.45	239	645 ± 20
PC 94	NA	NA	Hawaii	Petrel Cave	18.93	−12.92	208	625 ± 20
PC 95	NA	NA	Hawaii	Petrel Cave	16.9	−13.22	282	690 ± 20
PC 96A	NA	NA	Hawaii	Petrel Cave	15.29	−13.37	230	640 ± 20
PC 97	NA	NA	Hawaii	Petrel Cave	14.82	−13.78	216	630 ± 15
PC 98	NA	NA	Hawaii	Petrel Cave	17.2	−12.54	271	675 ± 15
PC 99	NA	NA	Hawaii	Petrel Cave	16.54	−12.3	225	635 ± 15
PC 99B	NA	NA	Hawaii	Petrel Cave	18.36	−12.88	234	640 ± 15
PC 100A	NA	NA	Hawaii	Petrel Cave	15.83	−13.2	261	665 ± 20
PC 100B	NA	NA	Hawaii	Petrel Cave	17.35	−13.86	241	645 ± 15
PC 101	NA	NA	Hawaii	Petrel Cave	15.73	−13.47	277	685 ± 15
PC 102	NA	NA	Hawaii	Petrel Cave	17.16	−13.14	1,701	2,170 ± 15
PC 103	NA	NA	Hawaii	Petrel Cave	15.25	−13.55	214	630 ± 20
PC 104	NA	NA	Hawaii	Petrel Cave	16.88	−12.92	383	795 ± 20
PC 105	NA	NA	Hawaii	Petrel Cave	15.27	−13.04	282	690 ± 20
PC 106	NA	NA	Hawaii	Petrel Cave	17.31	−12.59	246	650 ± 20
PC 107	NA	NA	Hawaii	Petrel Cave	16.38	−13.9	271	675 ± 15
PC 108	NA	NA	Hawaii	Petrel Cave	16.3	−14.19	234	640 ± 15

Sample ID	Museum	Catalog	Island	Location	δ^{15}N (‰)	δ^{13}C (‰)	Median age (B.P.)	^{14}C age (B.P.)
PC 109	NA	NA	Hawaii	Petrel Cave	17.53	−13.2	278	685 ± 20
PC 96B	NA	NA	Hawaii	Petrel Cave	17	−13.5	431	835 ± 15
UMI-08–1	NA	NA	Hawaii	Umii Manu	17.52	−12.42	248	650 ± 15
UMI-08–2	NA	NA	Hawaii	Umii Manu	15.49	−13.83	460	870 ± 15
UMI-08–3	NA	NA	Hawaii	Umii Manu	16.75	−14.21	3,058	3,290 ± 20
NMNH-08–19	NA	NA	Hawaii	Palisades Cave	16.13	−13.37	266	670 ± 20
NMNH-08–20	NA	NA	Hawaii	Palisades Cave	15.64	−13.28	160	575 ± 15
HFJ09.06	NA	NA	Hawaii	South Point	20.03	−13.73	216	630 ± 15
HFJ09.07	NA	NA	Hawaii	South Point	16.57	−13.64	294	705 ± 15
HFJ09.08	NA	NA	Hawaii	Jeffery's Cave	18.24	−12.68	2,660	2,925 ± 15
HFJ09.10	NA	NA	Hawaii	Old Fish and Wildlife Service camp Cave	17.59	−12.54	1,783	2,240 ± 15
HFJ09.11	NA	NA	Hawaii	Old Fish and Wildlife Service camp Cave	16.32	−13.85	1,515	2,015 ± 20
HFJ09.12	NA	NA	Hawaii	Kalahiki Cave System	18.45	−12.65	2,057	2,475 ± 20
HFJ09.14	NA	NA	Hawaii	Kiholo Bay	17.52	−12.41	323	730 ± 20
HFJ09.15	NA	NA	Hawaii	Kiholo Bay	18.08	−12.86	282	690 ± 20
HFJ09.16	NA	NA	Hawaii	Makalawena Cave System	16.04	−13.48	408	815 ± 15
HFJ09.17	NA	NA	Hawaii	Makalawena Cave System	16.37	−13.99	408	815 ± 15
HFJ09.18	NA	NA	Hawaii	Puuanahulu Cave N of Kioea Cave	15.96	−12.95	439	845 ± 20
HFJ09.19	NA	NA	Hawaii	Puuanahulu Cave N of Kioea Cave	16.05	−13.28	394	805 ± 20
HFJ09.11	NA	NA	Hawaii	Cave N of Umi Heiau	16.47	−13.95	294	705 ± 15
HFJ09.21	NA	NA	Hawaii	Cave N of Umi Heiau	16.55	−13.33	300	710 ± 20
HFJ09.22	NA	NA	Hawaii	Puu Keanui Cave	16.38	−13.59	274	680 ± 20
HFJ09.23	NA	NA	Hawaii	Puu Keanui Cave	16.96	−13.26	246	650 ± 20
HFJ09.24	NA	NA	Hawaii	Fireplow Cave	15.74	−14.06	499	935 ± 20
HFJ09.25	NA	NA	Hawaii	Fireplow Cave	15.97	−13.61	400	810 ± 20
HFJ09.27	NA	NA	Hawaii	Fireplow Cave	14.66	−13.77	463	875 ± 15
HFJ-09–1	NA	NA	Lanai	Feather Cave	17.72	−11.52	994	1,505 ± 20
HFJ-09–2	NA	NA	Lanai	Feather Cave	17.41	−11.91	899	1,405 ± 20
HFJ-09–3	NA	NA	Lanai	Feather Cave	15.32	−13.67	1,088	1,585 ± 20
HFJ-09–4	NA	NA	Lanai	Feather Cave	16.53	−13.88	823	1,330 ± 20
HFJ-09–5	NA	NA	Lanai	Feather Cave	15.58	−13.46	1,014	1,525 ± 20
LA01	NA	NA	Maui	Lua Alala, Kanaio	16.79	−13.17	3,360	3,530 ± 20
LA05	NA	NA	Maui	Lua Alala, Kanaio	15.24	−12.59	855	1,365 ± 20
LA07	NA	NA	Maui	Lua Alala, Kanaio	17.51	−13.02	3,095	3,315 ± 25
LA014	NA	NA	Maui	Lua Alala, Kanaio	16.66	−13.05	1,788	2,245 ± 15
LA019	NA	NA	Maui	Lua Alala, Kanaio	15.69	−13.77	837	1,345 ± 25
LA020	NA	NA	Maui	Lua Alala, Kanaio	15.65	−13.13	1,702	2,170 ± 20
LA021	NA	NA	Maui	Lua Alala, Kanaio	15.77	−13.19	914	1,420 ± 20
LA022	NA	NA	Maui	Lua Alala, Kanaio	15.3	−13.69	955	1,465 ± 20
NMNH-08–11	NA	NA	Maui	Lua Lepo	15.03	−13.89	4,409	4,340 ± 15
NMNH-08–12	NA	NA	Maui	Lua Lepo	14.48	−13.76	4,192	4,185 ± 20
NMNH-08–13	NA	NA	Maui	Lua Lepo	16.96	−13.22	4,395	4,330 ± 20
NMNH-08–14	NA	NA	Maui	Lua Lepo	15.11	−13.41	2,228	2,605 ± 15
NMNH-08–18	NA	NA	Maui	Puu Naio	16.19	−13.26	555	1,015 ± 20
BSHP08.10	NA	NA	Oahu	50-Oa-B6-100C	15.52	−13.34	1,596	2,085 ± 15
BSHP08.11	NA	NA	Oahu	50-Oa-B6-100C	15.13	−12.85	1,150	1,640 ± 15
BSHP08.14	NA	NA	Oahu	Barbers Point; Site 9659	14.77	−13.08	852	1,360 ± 15
BSHP08.15	NA	NA	Oahu	Barbers Point; Site 9659	15.92	−13.21	1,321	1,835 ± 15
BSHP08.20	NA	NA	Oahu	Barbers Point; Site 9659	14.89	−13.11	1,213	1,700 ± 20
BSHP08.22	NA	NA	Oahu	50-Oa-B6-78	17.46	−12.63	2,639	2,915 ± 20
BSHP08.24	NA	NA	Oahu	50-Oa-B6-78	15.39	−12.92	1,144	1,635 ± 20
BSHP08.26	NA	NA	Oahu	50-Oa-B6-78	17.06	−13.22	2,584	2,875 ± 20
BSHP08.27	NA	NA	Oahu	50-Oa-B6-78	16.24	−13.6	1,342	1,860 ± 20
BSHP08.29	NA	NA	Oahu	50-Oa-B6-78	14.15	−13.59	1,596	2,085 ± 15
BSHP08.31	NA	NA	Oahu	50-Oa-B6-78	15.58	−12.24	2,022	2,445 ± 15
NMNH 2010.05	NA	NA	Oahu	50-Oa-B6-22	14.57	−13.39	1,381	1,900 ± 15
NMNH 2010.08	NA	NA	Oahu	50-Oa-B6-22	16.42	−13.56	1,862	2,310 ± 15
HFJ-2011–02	NA	NA	Oahu	Barber's Point Site 2706–22B	18.21	−11.97	1,845	2,295 ± 15
HFJ-2011–03	NA	NA	Oahu	Barber's Point Site 2706–22B	17.11	−13.41	1,230	1,720 ± 15
HFJ-2011–04	NA	NA	Oahu	Barber's Point Site 2706–22B	15.98	−13.13	1,075	1,575 ± 15

Table S3.　Cont.

Sample ID	Museum	Catalog	Island	Location	δ^{15}N (‰)	δ^{13}C (‰)	Median age (B.P.)	^{14}C age (B.P.)
NMNH-08–2	NA	NA	Oahu	50-Oa-B6-22	16.69	−13.27	861	1,370 ± 15
NMNH-08–3	NA	NA	Oahu	50-Oa-B6-22	14.97	−13.41	1,643	2,125 ± 15
NMNH-08–4	NA	NA	Oahu	50-Oa-B6-22	14.86	−12.57	823	1,330 ± 15
NMNH-08–8	NA	NA	Oahu	50-Oa-B6-22	15.31	−13.14	1,756	2,215 ± 15
NMNH-08–9	NA	NA	Oahu	50-Oa-B6-22	14.6	−13.86	1,076	1,575 ± 15
BSHOP08.21	NA	NA	Oahu	Barber's Point, Site 9659	14.86	−13.45	1,420	1,930 ± 20
BSHP08.04	NA	NA	Oahu	50-Oa-B6-100C	17.07	−13.55	1,049	1,555 ± 20
BSHP08.07	NA	NA	Oahu	50-Oa-B6-100C	13.92	−13.26	1,150	1,640 ± 15
BSHP08.08	NA	NA	Oahu	50-Oa-B6-100C	15.27	−12.98	2,040	2,460 ± 20
NMNH-08–1	NA	NA	Oahu	50-Oa-B6-22	16.63	−13.68	846	1,355 ± 20
NMNH-08–5	NA	NA	Oahu	50-Oa-B6-22	15.02	−13.18	1,709	2,175 ± 15

In some cases, multiple subfossil bones were assigned the same catalog number, but only one element (e.g., left humerus) was sampled from each bone assemblage to prevent duplicate sampling. Catalog indicates the institution's catalog number, and location indicates site where bone was discovered. BPBM, Bernice Pauahi Bishop Museum; NA, not applicable; NMNH, National Museum of Natural History; USNM, United States National Museum.

Table S4. Isotope values and museum specimen information for Hawaiian petrel feather samples and modern and historic bone samples

Lab code	Museum	Catalog	Island	δ^{15}N (‰)	δ^{13}C (‰)	Age	SOI
DP.64.PF5	BPBM	183557	Kauai	11.11	−16.14	HY	−0.35
DP.64.PF4	BPBM	X-157513	Kauai	11.91	−16.67	HY	−.065
DP.35.PF49	USNM	639495	Kauai	14.91	−15.58	A	−2.38
DP.35.PF50	USNM	639502	Kauai	11.36	−16.71	HY	1.9
DP.35.PF105	USNM	639501	Kauai	11.50	−16.55	HY	−1.12
DP.35.PF240	USNM	643238	Maui	12.07	−15.02	A	2.25
DP.35.PF242	USNM	643236	Maui	14.14	−15.21	A	−2.05
DP.35.PF246	USNM	643235	Maui	12.01	−15.35	A	−2.05
DP.35.PF52	USNM	639504	Maui	11.36	−17.17	HY	−1.58
DP.35.PF53	USNM	639503	Maui	11.54	−17.10	HY	0.2
DP.35.PF103	USNM	639498	Maui	12.32	−17.40	HY	−1.48
DP.35.PF248	USNM	643246	Maui	12.33	−17.24	HY	−1.12
DP.35.PF1	NA	NA	Hawaii	14.76	−15.64	A	−1.6
DP.35.PF6	NA	NA	Hawaii	17.55	−16.38	A	0.45
DP.35.PF12	NA	NA	Hawaii	16.64	−15.96	A	0.45
DP 35 PF13	NA	NA	Hawaii	15.40	−15.37	A	1.88
DP.35.PF15	NA	NA	Hawaii	17.15	−15.77	A	1.88
DP.35.PF16	NA	NA	Hawaii	16.07	−16.26	A	−2.38
DP.35.PF20	NA	NA	Hawaii	15.82	−15.78	A	0.45
DP.35.PF21	NA	NA	Hawaii	15.85	−15.68	A	0.45
DP.35.PF22	NA	NA	Hawaii	16.75	−16.02	A	0.45
DP.35.PF25	NA	NA	Hawaii	12.98	−14.76	A	0.45
DP.35.PF36	NA	NA	Hawaii	13.68	−14.93	A	−1.02
DP.35.PF38	NA	NA	Hawaii	14.10	−14.59	A	−1.02
DP.35.PF40	NA	NA	Hawaii	15.53	−15.36	A	−1.02
DP.35.PF26	NA	NA	Hawaii	15.44	−15.42	A	−0.8
DP.35.PF3	NA	NA	Hawaii	12.66	−15.96	HY	−2.6
DP.35.PF8	NA	NA	Hawaii	15.75	−15.74	HY	−1.12
DP.35.PF9	NA	NA	Hawaii	16.32	−15.98	HY	−1.12
DP.35.PF10	NA	NA	Hawaii	15.84	−15.67	HY	1.92
DP.35.PF11	NA	NA	Hawaii	16.68	−15.23	HY	0.45
DP.35.PF18	NA	NA	Hawaii	15.79	−15.55	HY	−1.12
DP 35 PF19	NA	NA	Hawaii	15.47	−16.25	HY	−1.12
DP.35.PF46	NA	NA	Kauai	11.90	−15.24	A	0.45
DP.35.PF181	NA	NA	Kauai	12.42	−14.92	A	0.45
DP.35.PF182	NA	NA	Kauai	10.89	−15.23	A	0.45
DP 35 PF186	NA	NA	Kauai	11.54	−14.97	A	2.45
DP 35 PF187	NA	NA	Kauai	10.59	−15.58	A	2.45
DP 35 PF188	NA	NA	Kauai	12.12	−14.91	A	2.45
DP 35 PF189	NA	NA	Kauai	16.24	−15.49	A	2.45
DP 35 PF191	NA	NA	Kauai	14.44	−15.42	A	2.45
DP 35 PF192	NA	NA	Kauai	12.18	−14.74	A	2.45
DP 35 PF193	NA	NA	Kauai	13.69	−15.41	A	2.45
DP 35 PF194	NA	NA	Kauai	14.21	−16.12	A	2.45
DP 35 PF195	NA	NA	Kauai	11.08	−17.25	A	2.45
DP.35.PF51	NA	NA	Kauai	10.89	−16.62	HY	0.45
DP.35.PF54	NA	NA	Kauai	11.29	−16.80	HY	0.45
DP.35.PF205	NA	NA	Kauai	12.2	−17.5	HY	−1.28
DP.35.PF206	NA	NA	Kauai	12.3	−17.5	HY	−1.28
DP.35.PF207	NA	NA	Kauai	11.8	−17.3	HY	−1.28
DP.35.PF150	NA	NA	Kauai	11.32	−17.72	HY	−1.08
DP.35.PF178	NA	NA	Kauai	12.49	−17.11	HY	−1.08
DP.35.PF179	NA	NA	Kauai	12.19	−16.53	HY	−1.08
DP.35.PF114	NA	NA	Lanai	17.11	−15.25	A	2.95
DP.35.PF115	NA	NA	Lanai	16.85	−15.18	A	−0.8
DP.35.PF118	NA	NA	Lanai	14.68	−15.40	A	0.45
DP.35.PF122	NA	NA	Lanai	15.96	−15.70	A	0.45
DP.35.PF123	NA	NA	Lanai	14.64	−15.34	A	0.45
DP.35.PF125	NA	NA	Lanai	16.23	−15.88	A	−0.8
DP.35.PF126	NA	NA	Lanai	15.35	−15.34	A	−0.8
DP.35.PF152	NA	NA	Lanai	14.96	−15.81	A	2.95
DP.35.PF154	NA	NA	Lanai	16.14	−15.52	A	0.45

Table S4.   Cont.

Lab code	Museum	Catalog	Island	δ¹⁵N (‰)	δ¹³C (‰)	Age	SOI
DP.35.PF231	NA	NA	Lanai	16.87	−15.74	A	2.95
DP.35.PF233	NA	NA	Lanai	16.1	−15.83	A	2.95
DP.35.PF234	NA	NA	Lanai	16.04	−15.38	A	2.95
DP.35.PF236	NA	NA	Lanai	12.53	−15.71	A	2.95
DP.35.PF237	NA	NA	Lanai	15.88	−15.41	A	2.95
DP.35.PF238	NA	NA	Lanai	15.39	−15.24	A	NA
DP.35.PF43	NA	NA	Lanai	15.83	−14.66	A	−0.8
DP.35.PF44	NA	NA	Lanai	16.83	−15.41	A	−0.8
DP.35.PF232	NA	NA	Mau	12.3	−15.19	A	2.08
DP.35.PF180	NA	NA	Maui	15.74	−15.91	A	−1.3
DP.35.PF199	NA	NA	Maui	14.36	−14.86	A	2.25
DP.35.PF201	NA	NA	Maui	12.17	−15.27	A	2.08
DP.35.PF204	NA	NA	Maui	18.29	−15.51	A	2.25
DP.35.PF250	NA	NA	Maui	14.37	−15.42	A	2.25
DP.35.PF41	NA	NA	Maui	15.78	−14.95	A	−1.3
DP.35.PF148	NA	NA	Maui	13.61	−15.24	A	2.08
DP.35.PF200	NA	NA	Maui	14.78	−14.97	A	2.08
DP.35.PF202	NA	NA	Maui	12.86	−17.96	A	−2.05
DP.35.PF127	NA	NA	Maui	11.77	−17.73	HY	0.68
DP.35.PF128	NA	NA	Maui	12.66	−17.69	HY	0.68
DP.35.PF129	NA	NA	Maui	11.89	−17.40	HY	0.68
DP 35 PF139	NA	NA	Maui	11.69	−16.28	HY	2.08
DP.35.PF165	NA	NA	Maui	10.99	−17.39	HY	2.08
DP.35.B12	NA	NA	Hawaii	13.02	−14.47	A	NA
DP.35.B14	NA	NA	Hawaii	14.51	−14.58	A	NA
DP.35.B15	NA	NA	Hawaii	15.02	−14.12	A	NA
DP.35.B16	NA	NA	Hawaii	14.66	−14.75	A	NA
DP.35.B20	NA	NA	Hawaii	14.68	−14.18	A	NA
DP.35.B21	NA	NA	Hawaii	14.41	−15.31	A	NA
DP.35.B22	NA	NA	Hawaii	15.94	−14.61	A	NA
DP.35.B24	NA	NA	Hawaii	16.25	−13.89	A	NA
DP.35.B25	NA	NA	Hawaii	13.96	−14.52	A	NA
DP.35.B29	NA	NA	Hawaii	13.55	−14.54	A	NA
DP.35.B34	NA	NA	Hawaii	16.93	−15.03	A	NA
DP.35.B6	NA	NA	Hawaii	13.93	−14.95	A	NA
DP.35.B82	NA	NA	Hawaii	16.12	−13.21	A	NA
DP.35.B91	NA	NA	Hawaii	14.41	−15.28	A	NA
DP.35.B93	NA	NA	Hawaii	14.34	−15.13	A	NA
DP.35.B94	NA	NA	Hawaii	14.94	−14.29	A	NA
DP.35.B99	NA	NA	Hawaii	14.08	−15.27	A	NA
DP.35.B154	NA	NA	Hawaii	14.08	−14.56	A	NA
DP.35.B10	NA	NA	Hawaii	15.18	−14.93	HY	NA
DP.35.B11	NA	NA	Hawaii	13.75	−14.79	HY	NA
DP.35.B18	NA	NA	Hawaii	14.45	−15.31	HY	NA
DP.35.B27	NA	NA	Hawaii	15.02	−14.11	HY	NA
DP.35.B39	NA	NA	Hawaii	15.63	−14.04	HY	NA
DP.35.B8	NA	NA	Hawaii	15.69	−13.73	HY	NA
DP.35.B9	NA	NA	Hawaii	14.01	−14.29	HY	NA
DP.35.B92	NA	NA	Hawaii	14.53	−14.81	HY	NA
DP.35.B95	NA	NA	Hawaii	13.14	−14.03	UN	NA
DP.35.B96	NA	NA	Hawaii	14.72	−14.16	UN	NA
DP.35.B97	NA	NA	Hawaii	14.75	−15.47	UN	NA
DP.35.B98	NA	NA	Hawaii	14.35	−14.65	UN	NA
DP.35.B114	NA	NA	Lanai	13.44	−14.76	A	NA
DP.35.B115	NA	NA	Lanai	13.86	−15.45	A	NA
DP.35.B116	NA	NA	Lanai	13.85	−15.5	A	NA
DP.35.B117	NA	NA	Lanai	14.23	−14.95	A	NA
DP.35.B118	NA	NA	Lanai	13.34	−14.51	A	NA
DP.35.B119	NA	NA	Lanai	13.27	−14.48	A	NA
DP.35.B120	NA	NA	Lanai	13.305	−14.50	A	NA
DP.35.B122	NA	NA	Lanai	14.16	−14.04	A	NA
DP.35.B123	NA	NA	Lanai	14.55	−14.94	A	NA

Table S4. Cont.

Lab code	Museum	Catalog	Island	δ^15N (‰)	δ^13C (‰)	Age	SOI
DP.35.B126	NA	NA	Lanai	13.69	−14.9	A	NA
DP.35.B152	NA	NA	Lanai	14.88	−13.94	A	NA
DP.35.B154	NA	NA	Lanai	14.08	−14.56	A	NA
DP.35.B43	NA	NA	Lanai	13.63	−15.63	A	NA
DP.35.B44	NA	NA	Lanai	14.21	−15.16	A	NA
DP.35.B55	NA	NA	Lanai	14.75	−15.16	A	NA
DP.35.B41	NA	NA	Maui	13.28	−16.02	A	NA
DP.35.B244	NA	NA	Maui	13.61	−15.25	A	NA
DP.35.B252	NA	NA	Maui	13.01	−14.93	A	NA
DP.35.B241	NA	NA	Maui	15.05	−14.4	A	NA
DP.35.B250	NA	NA	Maui	15.87	−14.34	A	NA
DP.35.B148	NA	NA	Maui	16.33	−14.19	A	NA
DP.35.B242	NA	NA	Maui	13.56	−14.19	A	NA
DP.35.B255	NA	NA	Maui	13.95	−15.55	A	NA
DP.35.B258	NA	NA	Maui	13.15	−14.51	A	NA
DP.35.B240	NA	NA	Maui	14.29	−14.15	A	NA
DP 35 B147	NA	NA	Maui	15.17	−15.44	A	NA
DP 35 B45	NA	NA	Maui	14.18	−15.24	A	NA
DP.03.188	LACM	20266	Molokai	16.55	−12.99	A	NA
DP.03.187	LACM	20267	Molokai	14.71	−13.62	A	NA
DP.03.186	LACM	20268	Molokai	15.48	−13.44	A	NA
DP.03.189	LACM	20269	Molokai	19.01	−13.23	A	NA
DP.03.190	LACM	20270	Molokai	15.87	−13.43	A	NA
DP.03.191	LACM	20271	Molokai	15.64	−13.19	A	NA
DP.03.192	LACM	20272	Molokai	11.71	−13.08	A	NA
DP.03.193	LACM	20280	Molokai	16.73	−12.99	A	NA
DP.03.194	LACM	20281	Molokai	17.57	−13.43	A	NA
DP.03.195	LACM	20282	Molokai	15.47	−13.57	A	NA

Catalog indicates the institution's catalog number, and age classes are abbreviated as A (adult), HY (hatch-year bird), and UN (unknown). SOI indicates the Southern Oscillation Index values used in statistical analyses (see *Materials and Methods*). δ^13C values are shown before a correction for the Suess Effect. BPBM, Bernice Pauahi Bishop Museum; LACM, Natural History Museum of Los Angeles; NA, not applicable; USNM, United States National Museum.